

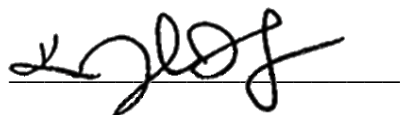
Dear Alexander Abramov,

We are pleased to inform you that your manuscript:

Local Electromechanical Characterization of Pr Doped BiFeO<sub>3</sub> Ceramics,  
by A.S. Abramov, D.O. Alikin, M.M. Neradovskiy, A.P. Turygin, A.D. Ushakov,  
R.O. Rokeah, A.V. Nikitin, D.V. Karpinsky, V.Ya. Shur, A.L. Kholkin

has been accepted for publication in the Proceedings of the International Conference  
"Scanning Probe Microscopy" (SPM-2017)  
in the special issue of *Ferroelectrics* journal (2018).

Managing Editor of the Taylor&Francis  
Kaleigh Sunday



27.11.2017



**Taylor & Francis**

Taylor & Francis Group

[www.taylorandfrancis.com](http://www.taylorandfrancis.com)

## **Local electromechanical characterization of Pr doped BiFeO<sub>3</sub> ceramics**

A. S. Abramov, D. O. Alikin, M. M. Neradovskiy, A. P. Turygin, A. D. Ushakov, R. O. Rokeah, A. V. Nikitin, D. V. Karpinsky, V. Ya. Shur, and A. L. Kholkin

### **QUERY SHEET**

This page lists questions we have about your paper. The numbers displayed at left can be found in the text of the paper for reference. In addition, please review your paper as a whole for correctness.

**Q1.** Au: Please cite Figure 4 in text.

### **TABLE OF CONTENTS LISTING**

The table of contents for the journal will list your paper exactly as it appears below:

Local electromechanical characterization of Pr doped BiFeO<sub>3</sub> ceramics  
**A. S. Abramov, D. O. Alikin, M. M. Neradovskiy, A. P. Turygin, A. D. Ushakov, R. O. Rokeah, A. V. Nikitin, D. V. Karpinsky, V. Ya. Shur, and A. L. Kholkin**



## Local electromechanical characterization of Pr doped BiFeO<sub>3</sub> ceramics

A. S. Abramov<sup>a</sup>, D. O. Alikin<sup>a,d</sup>, M. M. Neradovskiy<sup>a,b</sup>, A. P. Turygin<sup>a</sup>, A. D. Ushakov<sup>a</sup>,  
R. O. Rokeah<sup>a</sup>, A. V. Nikitin<sup>c</sup>, D. V. Karpinsky<sup>c</sup>, V. Ya. Shur<sup>a</sup>, and A. L. Kholkin<sup>a,d</sup>

- 5 <sup>a</sup>School of Natural Sciences and Mathematics, Ural Federal University, Ekaterinburg, Russia; <sup>b</sup>Université Côte d'Azur, CNRS, InPhyNi, Nice, France; <sup>c</sup>Scientific-Practical Materials Research Centre of NAS of Belarus, Minsk, Belarus; <sup>d</sup>Department of Physics & CICECO – Aveiro Institute of Materials, University of Aveiro, Aveiro, Portugal

10 Local electromechanical (EM) measurements were performed in Pr  
doped BiFeO<sub>3</sub> (BPFO) ceramics via piezoresponse force microscopy  
(PFM). The results revealed that local EM response was different from  
the macroscopic one due to the large contribution of the leakage  
current. The locally measured response was used to evaluate effective  
15 piezoelectric coefficient  $d_{33}$  of the material. The multi-frequency PFM  
mode with additional compensation of the cantilever-surface Coulomb  
interaction under application of the external DC bias provided the  
most accurate values of the effective  $d_{33}$  coefficient and allowed  
studying its surface distribution and residual depolarization field  
distribution across the surface of BPFO ceramics.

### ARTICLE HISTORY

Received 30 August 2017

Accepted 27 November 2017

### KEYWORDS

Bismuth ferrite; lead-free  
piezoelectric ceramics;  
electrostatic-free  
piezoresponse force  
microscopy

## 1. Introduction

The discovery of large remnant polarization in bismuth ferrite (BFO) thin films prepared by the pulsed laser deposition has been attracting researchers to study their piezoelectric and electromechanical (EM) properties for various applications in EM devices [1]. The main issue in the application of BFO-based ceramics is reduced phase stability and high electrical conductivity deteriorating the piezoelectric performance [2]. One of the solutions of this problem is the fabrication BFO-based materials at the compositionally driven morphotropic phase boundary (MPB), which could be done, for example, by the substitution with rare earth elements [3–7]. By the analogy, commercial Pb<sub>0.5</sub>Zr<sub>0.5</sub>TiO<sub>3</sub> solid solutions are commonly produced with the composition in the vicinity of MPB, which has been shown to drastically increase the EM response [8,9]. The MPB in BFO is relatively temperature independent and accompanied by the reduction of the elastic moduli and enhancement of piezoelectric response accompanied with simultaneous decrease of the coercive field [3]. The role of MPB is usually discussed in terms of the nanoscale phase coexistence beneficial for the polarization rotation and extension [8,9]. Moreover, doping by rare-earths elements has the potential to

**CONTACT** A. S. Abramov ✉ [alexander.abramov@urfu.ru](mailto:alexander.abramov@urfu.ru) School of Natural Sciences and Mathematics, Ural Federal University, 620000, Ekaterinburg, Russia.

Color versions of one or more of the figures in the article can be found online at [www.tandfonline.com/gfer](http://www.tandfonline.com/gfer).

© 2018 Taylor & Francis Group, LLC

stabilize perovskite phase in ceramic materials, decrease the secondary phases impurities and, as a consequence, reduce the leakage current [2,10]. The coexistence of structural phases is apparently accompanied by a decrease in the elastic moduli and, therefore, leads to improvement of the respective piezoelectric properties [11,12].

BFO ceramics doped by Pr (BPFO) have MPB in the range of doping degree  $x = 0.125 - 0.16$ . BPFO with Pr content up to  $x = 0.12$  were obtained in a polar rhombohedral  $R3c$  phase. The rhombohedral structure of BPFO for  $x = 0.12$  is stable at room temperature and no changes in X-ray diffraction patterns were detected after 2-month shelf time, while ceramics with  $x = 0.125$  exhibit an isothermal structural transformation at room temperature: approximately 10% of initial rhombohedral phase gradually transforms into an anti-polar ( $Pbam$  or  $Pnam$ ) one after 1-month shelf time [11,12]. The structure of the sample at  $x = 0.14$  has been refined in multi-phase state (polar and anti-polar states coexist). Ceramics with  $x \geq 16\%$  Pr were found to belong to a stable anti-polar phase [11,12]. Doping of BFO by Pr releases magnetization caused by the weak ferromagnetic state: small values of spontaneous magnetization exist at room temperature [13,14]. It was supposed that structural defects and/or local variations in the chemical composition could be a source of such behavior [15]. Spontaneous magnetization, notable piezoelectric coefficient, and dielectric permittivity make this composition perspective for the applications in magnetoelectric devices, too [16–20].

Due to the presence of various defects in the material, polarization hysteresis and piezoelectric measurements are typically supplemented with the big contribution of the leakage current. Only a few studies have been conducted and provided unambiguous data on the macroscopic EM performance and switching behavior [2]. Some authors used the values of piezoelectric coefficients obtained by local methods, such as piezoresponse force microscopy (PFM), in order to evaluate EM activity in BFO. Piezoresponse was measured either in arbitrary units or in cantilever deflection [12]. However, these methods are ambiguous because of the strong coupling of the inherent piezoelectric response with cantilever dynamics and electrostatic cantilever-surface interaction [21].

In this contribution, we focus on the comprehensive characterization of the piezoelectric response in BPFO using macroscopic laser interferometry and scanning probe microscopy (SPM) method realized in single frequency and multi-frequency PFM modes. We found significantly higher values of the effective  $d_{33}$  coefficient in the local studies, which we attributed to incomplete polarization of the ceramics due to the leakage current. We used a novel approach consisting of the additional electrostatic force compensation by the application DC bias voltage.

## 2. Experimental details

The investigated samples of BPFO ceramics with molar praseodymium concentration 12.5, 14, and 15% were produced using the two-stage solid phase synthesis [22]. The initial high purity oxides were taken in the stoichiometric ratio and thoroughly mixed for about 30 min in a planetary mill RETSCH PM-100 using high purity isopropyl alcohol as a medium. The synthesis temperature increased from 950 to 1050°C with increasing praseodymium content; the samples were quenched from the synthesis temperature down to room temperature. X-ray diffraction (XRD) measurements were made on Rigaku D/MAX-B diffractometer using Cu-K $\alpha$  radiation. The XRD data were processed by the Rietveld method using the FullProf software.

Samples surface was rigorously polished by means of diamond paste with decreasing powder size from 6 to 0.25  $\mu\text{m}$ . Final polishing was done with colloidal silica (SF1 Polishing Suspension, Logitech, United Kingdom).

80 For the macroscopic studies, ceramics were poled by the application of 2 kV/mm external electric field pulses of trapezium shape with duration 15 minutes, ramp and fall about 600 V/mm per min. It is important to note that application of electric field every time was accompanied by the leakage current in the nA range, so the real applied field could be different from the calculated based on nominal voltage applied.

85 Macroscopic measurements of the electromechanical response were done using precise single-beam laser Michelson interferometer with signal discrimination by the selective amplifier (lock-in) [23]. Solid state diode laser LCM-S-111-20-NP25 (Lasercompact, Russia) with wavelength 532 nm and power 20 mW and lock-in amplifier SR-830 (Stanford Research, USA) were used as key components of the interferometer.

90 PID-feedback loop for thermal drift stabilization was based on the piezo actuator P-841.01 and piezo controller E-709.SRG (Physik Instruments, Germany). Measurements were done in the frequency range of 1–100 kHz with 50 V driving amplitude. Piezoelectric coefficients were evaluated from the AC voltage sweep (1–50 V) at the flat regions of frequency dependencies as a linear coupling between displacement and  
95 applied voltage.

PFM measurements were realized with NanoLaboratory NTEGRA Aura (NT-MDT, Russia) by the MikroMasch NSC18/Pt probes with 30 nm tip radius, 75 kHz free resonance frequency and 2.8 N/m spring constant. Single- and multi-frequency regimes were exploited.

### **2.1. Single frequency out-of-resonance PFM (SF-PFM)**

100 SF-PFM measurements were performed using microscope internal electronics. 3 V, 21 kHz driving amplitude was applied to the SPM tip. Frequency of scanning was chosen far from the contact resonance frequency (400–500 kHz) in order to exclude all the cantilever dynamics inputs.

### **2.2. Band excitation multi-frequency PFM (BE-PFM)**

105 BE-PFM measurements were performed by the external electronics NI PXIe-1071 (National instruments, USA) with the built-in waveform generator (NI PXI-5421) and multifunction input-output module (NI PXI-6115). The sampling frequency of data acquisition and signal generation was 10 MS/s. The probing of contact resonance cantilever frequency (400–500 kHz) was done using 90 kHz-width window excitation with  
110 about 30 discrete frequency bins and 200–400 ms exposure time per point. The voltage amplitude per frequency bin was 2–5 V. More detailed description of the theoretical approach for the multi-frequency discrete bin band excitation method could be found in Ref. [24].

In order to nullify the parasitic inputs of the probe-surface electrostatic interaction,  
115 we used DC compensation of the surface potential [25]. Unfortunately, the SF-PFM noise level in the BPFO was found too big to reveal explicit dependence of the piezoresponse on the applied DC voltage. Only multi-frequency on-resonance regimes with x100–200 resonance amplification allowed implementing electrostatic force correction

algorithm [25]. We typically used 10 V DC bias to reveal the minima of the piezores-  
 120 ponce and exclude polarization reversal (Fig. 5). The reversibility of all the processes  
 was proved by the two-pass approach, where the EM signal was measured under the  
 DC voltage sweep.

Tip-induced polarization reversal was done using external NI-6251 multifunction Data  
 Acquisition board (National Instruments, USA) and high-voltage amplifier Trek-677B  
 125 (TREK Inc., USA). The commercial probes ScanSens HA\_FM/W2C Etalon with conductive  
 $W_2C$  coating, 35 nm radius of curvature, 114 kHz resonance frequency, and 6 N/m spring  
 constant. Local switching was done by writing the poling maps in a number of grains with  
 spontaneous polarization preferably out-of-plane oriented (maximal piezoresponse). The  
 effective radius of the created domains was calculated from the switched area in circular  
 130 approximation.

All measurements were performed in dry atmosphere (relative humidity 5–15%) provided  
 by constant dry airflow through the microscope chamber.

### 3. Results and discussion

#### 3.1. Macroscopic electromechanical response

135 The macroscopic poling of the samples was accompanied by the high leakage current, which is a  
 sign that actual poling voltage could be significantly smaller than the applied one. This could  
 result in only partial reorientation of spontaneous polarization in ceramics and smaller piezoelec-  
 tric response. For example, Sm doped BFO had the effective macroscopic piezoresponse increas-  
 ing with the applied voltage without any saturation [26]. It is interesting to note that we found a  
 140 general trend of piezoresponse increase with decreasing frequency. This effect was observed ear-  
 lier and attributed to non-linear Maxwell-Wagner relaxation [27,28] or hopping conductivity via  
 the defects [29]. In our case, the frequency range with detected amplification of the response was  
 about 20–30 kHz. This is quite important observation, because, typically, PFM out-of-resonance  
 signal is believed to be frequently independent in a frequency range far from the contact reso-  
 145 nance frequency (300–900 kHz for the stiff cantilevers – 3–15 N/m). This was not the case of our  
 measurements and could be a source of additional error for the values of the effective piezoelec-  
 tric coefficients. The approximate values of the effective  $d_{33}$  for all three samples were found to

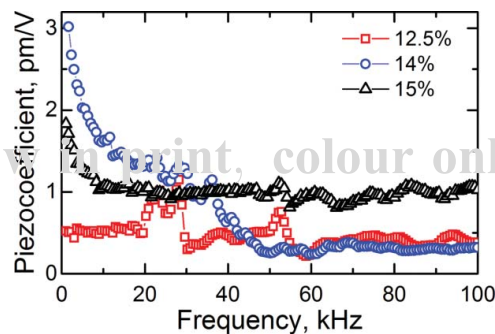


**Figure 1.** Frequency dependencies of the macroscopic EM response in PBFO measured by the laser interferometry.  $U_{ac} = 50$  V. The effective  $d_{33}$  value for the 70 kHz: 0.32 pm/V for BPFO 12.5%, 0.42 pm/V for BPFO 14%, 0.9 pm/V for BPFO 15%.

be quite small: about 0.5–1 pm/V (Fig. 1). Significant frequency dependence of the response does not allow comparing reliably the values of the piezoelectric coefficients. We supposed that this ambiguity could be due to the extensive leakage current impeding poling and contributing to EM response.

### 3.2. Domain structure and phase composition

The grain size in all three compositions of BPFO was about 8–12  $\mu\text{m}$ . PFM images from BPFO ceramics demonstrated coexistence of the two phases: piezoelectrically active, attributed to polar  $R3C$  phase (R-phase), and piezoelectrically inactive, attributed to the anti-polar  $Pbam$  or  $Pnam$  phase (O-phase) [11,12]. R-phase revealed a mixture of lamellar domains with non-180° domain walls and watermark areas exhibiting irregular shapes and separated by 180° walls (Fig. 2). PFM revealed fraction of the anti-polar phase increasing with doping (Fig. 2), which is in line with XRD data (Fig. 3). The reduction of the polar phase size with doping is responsible for the size effect, because the lamellar/watermark ratio decreased.

The PFM signal distribution made by SF-PFM and BE-PFM in BPFO ceramics was quite similar. The only difference was a big variability of the amplitude and phase in anti-polar phase, where band excitation usually fitted data in a wrong way due to the absence of the explicit contact resonance. Piezoresponse distribution was found to have a discrete set of the measured signals (contrasts): about 5–6 due to piezoresponse and one related to the averaged noise level. These contrasts were caused by the small variations of the PFM amplitude due to different orientations of spontaneous polarization in a multiaxial grain.

### 3.3. Evaluation of the local effective $d_{33}$ piezoelectric coefficient

Obviously, the influence of the leakage current through the different interfaces: domain walls phase and grain boundaries could be excluded completely only using local techniques for the

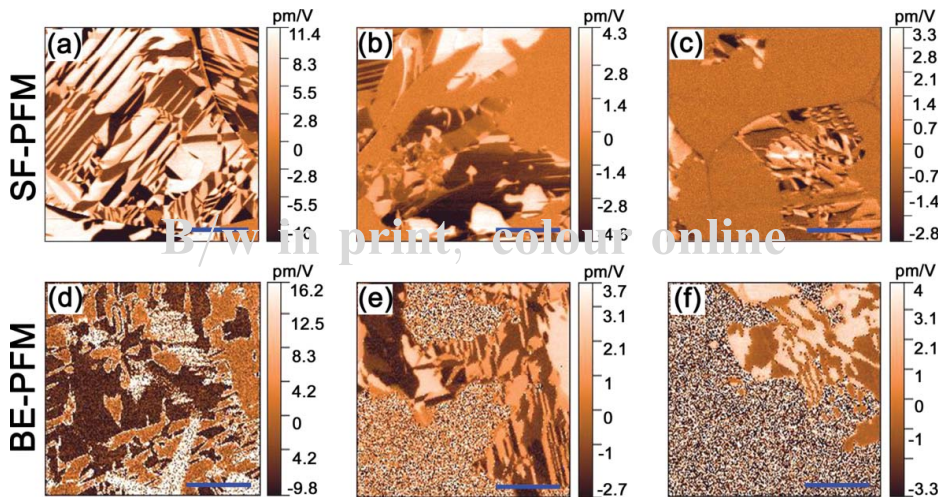


**Figure 2.** SF-PFM and BE-PFM images of the domain structure in BPFO ceramics with different compositions: (a), (b) 12.5%, (c), (d) 14%, (e), (f) 15%. The ruler length is 3  $\mu\text{m}$  equal for all images.



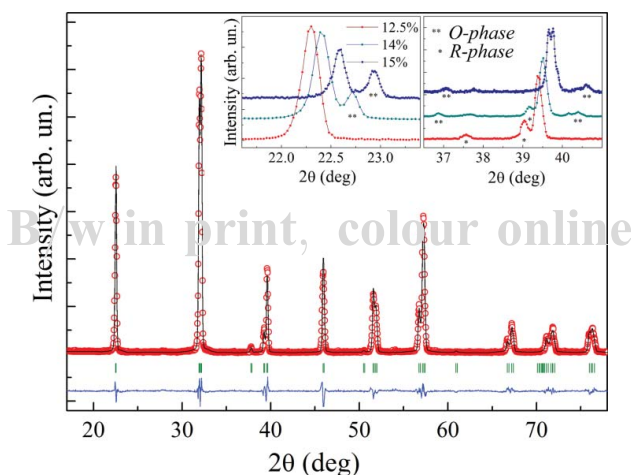


**Figure 3.** XRD spectrum of the BPFO 12.5% ceramics. On inset: evolution of the bands inherent for the R- and O-phases. The estimated fraction R to O phase is: BPFO 12.5% ~100%/0%, BPFO 14% ~15%/85%, BPFO 15% ~5%/95%.

measurements. That is why we used PFM to estimate quantitatively the locally measured  $d_{33}$  coefficient within the grains.

Actually, the quantitative measurements of local effective  $d_{33}$  are complicated because of stiffness calibration and sensitivity problems [30], cantilever dynamics contribution [31,32], parasitic effects (frequency dependent background) [25,33–35], etc. Nevertheless, several techniques could be used to correct the data and to explain the low values of the macroscopic response.

We realized quantification of the PFM signal by means of the probe sensitivity calibration using quasi-static force distance curves. The amplitude of the piezoelectric response across the scan was represented as a histogram and average effective  $d_{33}$  was extracted as a median of the signal distribution (Fig. 3).

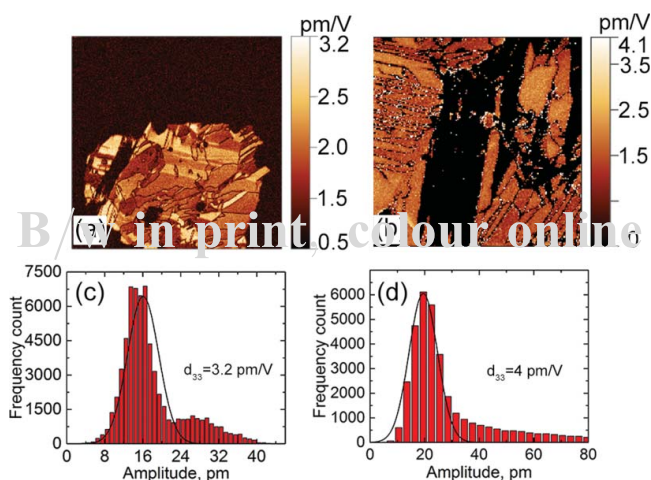


**Figure 4.** (a) SF-PFM (5V AC) and (b) BE-PFM (5V AC per bin) amplitude. (c) SF-PFM and (d) BE-PFM histogram of amplitude distribution across the image. (a) and (c) BPFO 15%; (b) and (d) BPFO 12.5%.



Then, the force distance curve was acquired and cantilever optical sensitivity calibration coefficient was extracted. The effective  $d_{33}$  coefficient in pm/V was calculated according to the following formula:

$$d_{33} = \frac{A[\text{pm}]}{V_{\text{mod}}[\text{V}]} = \frac{\text{InvOLS}[\frac{\text{nm}}{\text{nA}}] \times A[\text{nA}]}{V_{\text{mod}}[\text{V}]}, \quad (1)$$

185 where *InvOLS* is optical cantilever sensitivity,  $A_{\text{SF}}$  is the averaged amplitude value,  $V_{\text{mod}}$  is the value of the modulating voltage applied at scanning.

SF-measurements demonstrated decreasing trend in the piezoelectric performance, which is in line with crystal structure transformation. Nevertheless, the average error of the coefficient determination is quite high (about 30–40%). BE-PFM gave similar values and errors. 190 These could not be explained by the increased sensitivity of the method: BE-PFM has at least 100 times amplification due to measurements at contact resonance frequency. EM signal has more contributions either from cantilever dynamics input, or from additional “electrostatic” response, appeared as result of the local and distributed cantilever-surface interaction [25].

The first contribution, indeed, may have a big influence on the measured data [33]; however, we found that the used cantilevers were quite stiff and provided the contact stiffness 195 enough to make the data reliable [33].

The second contribution is more important for our case. The physical reason of “electrostatic contribution” is a cantilever-surface capacitance appearing as a result of non-local Coulomb forces or tip interaction with injected charge. Generally, stiffer cantilevers could be 200 used to remove the parasitic inputs from electrostatic ones; however, this approach has several disadvantages:

- quite big stiffness is necessary to make electrostatic response negligible [36];
- stiff cantilever can modify the surface mechanically or induce some electric field through electromechanical coupling [37];
- 205 • the contact resonance frequency shifts with cantilever stiffness and for stiff enough cantilever it could be in MHz range, where optical registration system becomes less sensitive.

That is why we expanded the so-called “electrostatic-free” PFM approach suggested by Kim [25] to the quantification of the response in the ferroelectric systems with non-trivial 210 domain structure and phase assemblages.

### 3.4. Influence of the electrostatic correction on the effective $d_{33}$ coefficients

“Electrostatic-free” PFM implies using additional DC bias to suppress surface potential and, therefore, minimize electrostatic responses (see Eq. (1)) in a way, how it is usually done in Kelvin probe force microscopy (KPFM). In contrast to the experiments performed by Kim, 215 we had more complicated problem due to inhomogeneity of the system and, consequently, distribution of the surface potential across the surface [25]. That is why we could not use the same applied bias for all scans and it had to be selected carefully for each scan point. We realized the other approach similar to the switching spectroscopy PFM widely used in PFM community [38,39]. In the frame of this approach, in each point of the scan we sweep DC 220 offset to obtained complete curve of the EM signal dependence on the DC voltage. It must be noted that the applied DC bias was smaller than the threshold voltage of the local

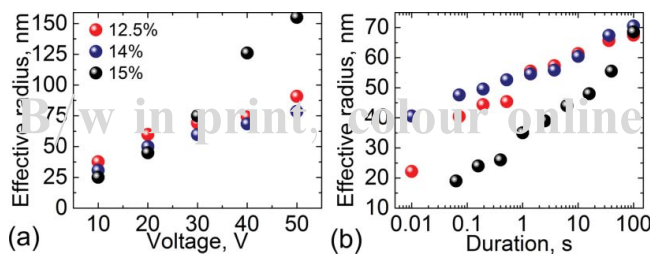


**Figure 5.** Local switching in PBFO ceramics with different composition: dependence of the effective domain radius on the (a) amplitude of voltage pulse and (b) duration of voltage pulse.

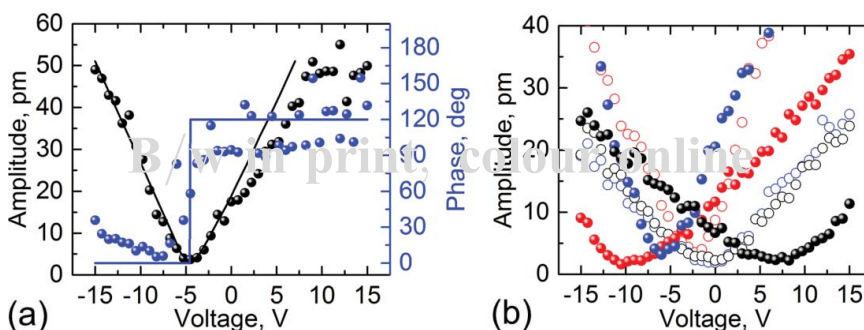


**Figure 6.** “Electrostatic-free” BE-PFM. (a) Typical PFM spectroscopy curve: PFM amplitude and phase vs DC bias, (b) PFM amplitude vs DC bias spectroscopy curve variation across the surface for different BPFO compositions: open symbols – curves with surface potential close to zero, filled symbols – curves with deviated surface potential.

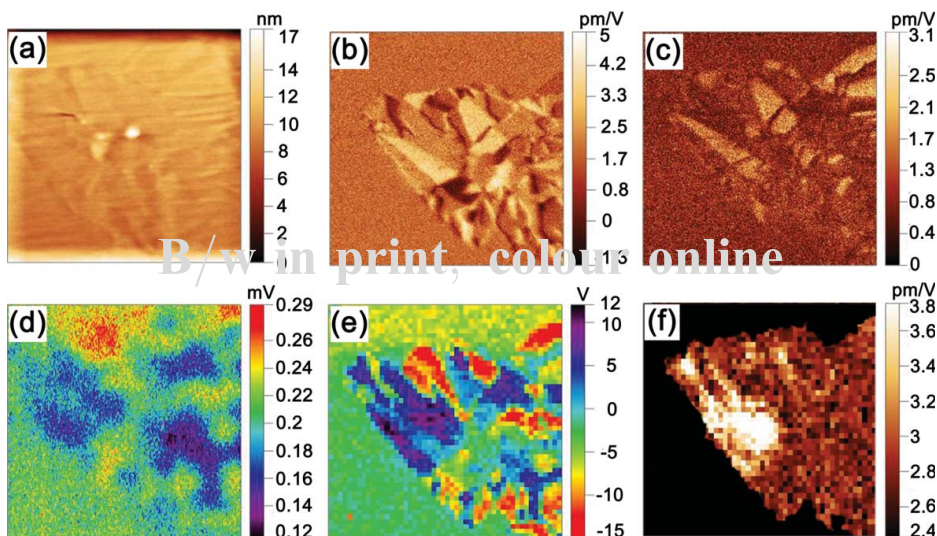


**Figure 7.** PFM with correction of electrostatic forces. (a) Topography, (b) surface potential measured by KPFM, (c) SF-PFM piezoresponse, (d) SF-PFM amplitude, (e) surface potential measured by PFM, (f) corrected PFM amplitude within R-phase areas.

**Table 1.** Effective  $d_{33}$  coefficients for BPFO ceramics with different compositions.

Method	Effective $d_{33}$ , pm/V		
	BPFO 12.5%	BPFO 14%	BPFO 15%
SF-PFM	$5.2 \pm 0.5$	$3.7 \pm 0.6$	$3.5 \pm 0.4$
BE-PFM	$4.4 \pm 0.7$	$3.5 \pm 0.4$	$3.4 \pm 0.7$
Band Excitation with compensation	$4.1 \pm 0.1$	$3.0 \pm 0.1$	$2.4 \pm 0.1$

polarization reversal: local switching did not reveal any irreversible domain structure change at the voltage smaller than 10 V (Fig. 5). Moreover, before and after scan the domain structure done in BE-PFM did not show any changes under the action of applied DC voltage.

225 Typical PFM spectroscopy curves measured under the DC sweep represented the V-shape in amplitude with phase inversion in the point with minimum response (Fig. 6a). Such behavior was reported earlier by Kim in lithium niobate single crystals and reliably described electrostatic forces [25]. The only difference with the case of KPFM is that the minimal signal does not lie at the noise level, but has a meaning of the corrected piezoelectric amplitude (piezoelectric amplitude without input of the electrostatic forces, see the first term in Eq. (1)).

230 Mapping the PFM spectroscopy curves across the surface demonstrated various experimental situations: the minima close to the 0 V bias — no “electrostatic” input and minima shifted to the positive of negative voltage — “electrostatic” input. For the quantification of the data, we averaged the minima across the number of the surface scans and found considerable decrease of the effective  $d_{33}$  values. The corrected values of the effective  $d_{33}$  were found to be quite similar in BPFO 14% and BFO 15%, while the BFO 12.5% exhibited in R-phase had higher  $d_{33}$  values, which showed higher Pr doping to trend negatively on the piezoelectric coefficient.

240 We analyzed also surface distribution of the applied DC offset correspondent to minimum of PFM amplitude and corrected PFM amplitude (Fig. 7). The DC offset applied to sample had the same meaning as in the contact KPFM discussed earlier in literature [40]. This was proved by the similarity of surface potential data obtained by KPFM technique (Fig. 7b). The only difference was an enhancement of resolution and signal level. The contrast obtained in the KPFM data had a correlation with the domain structure and we addressed it to screening charges [41]. The corrected PFM amplitude revealed also some variation correlated with domains and domain wall positions, but had small deviation, possibly due to negligible variation of the effective  $d_{33}$  coefficient.

#### 4. Conclusion

250 We conducted a comprehensive study of the electromechanical performance in BPFO ceramics of different compositions around MPB by the laser interferometry and piezoresponse force microscopy. The macroscopic data demonstrated quite small (and similar) values of the electromechanical response in all ceramics, while PFM revealed essential difference depending on Pr content. Single frequency and multi-frequency regimes of PFM were compared and it was shown that the most reliable data were obtained in multi-frequency on-resonance measurements with additional application of DC bias compensating the cantilever-surface electrostatic interaction. The variation of the surface potential due to

electric field produced by screening charges provided considerably higher electromechanical response. Developed approach of the “electrostatic-free” PFM allowed distinguishing the piezoelectric response and Coulomb tip-surface interaction. The surface potential and effective  $d_{33}$  distribution across the surface were visualized simultaneously. Proposed approach is valuable for the characterization of the various inhomogeneous ferroelectric materials: multiaxial and multi-domain single crystals, ceramics, and thin films.

## Acknowledgment

The equipment of the Ural Center for Shared Use “Modern nanotechnology” was used. The reported study was funded by RFBR (grant No. 17–52-04074) and BRFFR (grant No. F17RM-036). This work was developed within the scope of the project CICECO-Aveiro Institute of Materials, POCI-01-0145-FEDER-007679 (FCT Ref. UID/CTM/50011/2013), financed by national funds through the FCT/MEC and when appropriate co-financed by FEDER under the PT2020 Partnership Agreement. This project has received funding from the European Union’s Horizon 2020 research and innovation program under the Marie Skłodowska-Curie grant agreement No 778070.

## Funding

European Union’s Horizon 2020 research and innovation program, Marie Skłodowska-Curie grant agreement No 778070 CICECO-Aveiro Institute of Materials, POCI-01-0145-FEDER-007679, UID/CTM/50011/2013 RFBR, 17-52-04074

## References

- [1] J. Wang, J. B. Neaton, H. Zheng, V. Nagarajan, S. B. Ogale, B. Liu, D. Viehland, V. Vaithyanathan, D. G. Schlom, U. V. Waghmare, N. A. Spaldin, K. M. Rabe, M. Wuttig, R. Ramesh, Epitaxial  $\text{BiFeO}_3$  multiferroic thin film heterostructures. *Science*. **299**, 1719–1722 (2003).
- [2] T. Rojac, A. Benčan, B. Malič, G. Tutuncu, J. L. Jones, J. E. Daniels, D. Damjanovic,  $\text{BiFeO}_3$  ceramics: Processing, electrical, and electromechanical properties. *J Am Ceram Soc*. **97**, 1993–2011 (2014).
- [3] S. Fujino, M. Murakami, V. Anbusathaiah, S. H. Lim, V. Nagarajan, C. J. Fennie, M. Wuttig, L. Salamanca-Riba, I. Takeuchi, Combinatorial discovery of a lead-free morphotropic phase boundary in a thin-film piezoelectric perovskite. *Appl Phys Lett*. **92**, 82–85 (2008).
- [4] D. Kan, L. Pálová, V. Anbusathaiah, C. J. Cheng, S. Fujino, V. Nagarajan, K. M. Rabe, I. Takeuchi, Universal behavior and electric-field-induced structural transition in rare-earth-substituted  $\text{BiFeO}_3$ . *Adv Funct Mater*. **20**, 1108–1115 (2010).
- [5] J. Walker, H. Simons, D. O. Alikin, A. P. Turygin, V. Y. Shur, A. L. Kholkin, H. Ursic, A. Bencan, B. Malic, V. Nagarajan, T. Rojac, Dual strain mechanisms in a lead-free morphotropic phase boundary ferroelectric. *Sci Rep*. **6**, 19630 (2016).
- [6] V. A. Khomchenko, D. A. Kiselev, M. Kopcewicz, M. Maglione, V. V. Shvartsman, P. Borisov, W. Kleemann, A. M. L. Lopes, Y. G. Pogorelov, J. P. Araujo, R. M. Rubinger, N. A. Sobolev, J. M. Vieira, A. L. Kholkin, Doping strategies for increased performance in  $\text{BiFeO}_3$ . *J Magn Magn Mater*. **321**, 1692–1698 (2009).
- [7] I. O. Troyanchuk, D. V. Karpinsky, M. V. Bushinsky, O. S. Mantyskaya, N. V. Tereshko, V. N. Shut, Phase transitions, magnetic and piezoelectric properties of rare-earth-substituted  $\text{BiFeO}_3$  ceramics. *J Am Ceram Soc*. **94**, 4502–4506 (2011).
- [8] A. Ghosh, D. Damjanovic, Antiferroelectric–ferroelectric phase boundary enhances polarization extension in rhombohedral  $\text{Pb}(\text{Zr,Ti})\text{O}_3$ . *Appl Phys Lett*. **99**, 232906 (2011).
- [9] D. A. Damjanovic, Morphotropic phase boundary system based on polarization rotation and polarization extension. *Appl Phys Lett*. **97**, 2008–2011 (2010).

- [10] S. Karimi, I. M. Reaney, Y. Han, J. Pokorny, I. Sterianou, Crystal chemistry and domain structure of rare-earth doped BiFeO<sub>3</sub> ceramics. *J Mater Sci.* **44**, 5102–5112 (2009).
- 305 [11] D. V. Karpinsky, I. O. Troyanchuk, V. Sikolenko, V. Efimov, E. Efimova, M. Willinger, A. N. Salak, A. L. Kholkin, Phase coexistence in Bi<sub>1-x</sub>Pr<sub>x</sub>FeO<sub>3</sub> ceramics. *J Mater Sci.* **49**, 6937–6943 (2014).
- [12] D. V. Karpinsky, I. O. Troyanchuk, V. V. Sikolenko, V. Efimov, E. Efimova, M. V. Silibin, G. M. Chobot, E. Willinger, Temperature evolution of the crystal structure of Bi<sub>1-x</sub>Pr<sub>x</sub>FeO<sub>3</sub> solid solutions. *Phys Solid State.* **56**, 2263–2268 (2014).
- 310 [13] V. A. Khomchenko, I. O. Troyanchuk, D. V. Karpinsky, J. A. Paixão, Structural and magnetic phase transitions in Bi<sub>1-x</sub>Pr<sub>x</sub>FeO<sub>3</sub> perovskites. *J Mater Sci.* **47**, 1578–1581 (2011).
- [14] S. T. Zhang, M. H. Lu, D. Wu, Y. F. Chen, N. B. Ming, Larger polarization and weak ferromagnetism in quenched BiFeO<sub>3</sub> ceramics with a distorted rhombohedral crystal structure. *Appl Phys Lett.* **87**, 1–3 (2005).
- 315 [15] D. V. Karpinsky, I. O. Troyanchuk, O. S. Mantyskaya, V. A. Khomchenko, A. L. Kholkin, Structural stability and magnetic properties of Bi<sub>1-x</sub>La(Pr)<sub>x</sub>FeO<sub>3</sub> solid solutions. *Solid State Commun.* **151**, 1686–1689 (2011).
- [16] M. Wu, W. Wang, X. Jiao, G. Wei, L. He, S. Han, Y. Liu, D. Chen, Structural and multiferroic properties of Pr and Ti co-doped BiFeO<sub>3</sub> ceramics. *Ceram Int.* **42**, 14675–14678 (2016).
- 320 [17] P. He, Z. L. Hou, C. Y. Wang, Z. J. Li, J. Jing, S. Bi, Mutual promotion effect of Pr and Mg co-substitution on structure and multiferroic properties of BiFeO<sub>3</sub> ceramic. *Ceram Int.* **43**, 262–267 (2017).
- [18] I. Coondoo, N. Panwar, I. Bdikin, V. S. Puli, R. S. Katiyar, A. L. Kholkin, Structural, morphological: Piezoresponse studies of Pr and Sc co-substituted BiFeO<sub>3</sub> ceramics. *J Phys D Appl Phys.* **45**, 55302 (2012).
- 325 [19] P. C. Sati, M. Arora, S. Chauhan, S. Chhoker, Structural, magnetic, and optical properties of Pr and Zr codoped BiFeO<sub>3</sub> multiferroic ceramics. *J Appl Phys.* **112**, 094102 (2012).
- [20] J. V. Vidal, A. V. Turutin, I. V. Kubasov, M. D. Malinkovich, Y. N. Parkhomenko, S. P. Kobeleva, A. L. Kholkin, N. A. Sobolev, Equivalent magnetic noise in magnetoelectric laminates comprising bidomain LiNbO<sub>3</sub> crystals. *IEEE Trans Ultrason Ferroelectr Freq Control.* **64**, 1102–1119 (2017).
- 330 [21] N. Balke, P. Maksymovych, S. Jesse, A. Herklotz, A. Tselev, C. B. Eom, I. I. Kravchenko, P. Yu, S. V. Kalinin, Differentiating ferroelectric and nonferroelectric electromechanical effects with scanning probe microscopy. *ACS Nano.* **9**, 6484–6492 (2015).
- 335 [22] D. V. Karpinsky, I. O. Troyanchuk, M. Tovar, V. Sikolenko, V. Efimov, A. L. Kholkin, Evolution of crystal structure and ferroic properties of La-doped BiFeO<sub>3</sub> ceramics near the rhombohedral-orthorhombic phase boundary. *J Alloys Compd.* **555**, 101–107 (2013).
- [23] A. D. Ushakov, E. Mishuk, E. Makagon, D. O. Alikin, A. A. Esin, I. S. Baturin, A. Tselev, V. Y. Shur, I. Lubomirsky, A. L. Kholkin, Electromechanical properties of electrostrictive CeO<sub>2</sub>:Gd membranes: Effects of frequency and temperature. *Appl Phys Lett.* **110**, 142902 (2017).
- 340 [24] K. Romanyuk, S. Y. Luchkin, M. Ivanov, A. Kalinin, A. L. Kholkin, Single- and multi-frequency detection of surface displacements via scanning probe microscopy. *Microsc Microanal.* 1–10 (2015).
- 345 [25] S. Kim, D. Seol, X. Lu, M. Alexe, Y. Kim, Electrostatic-free piezoresponse force microscopy. *Nat Publ Gr.* **7**, 41657 (2017).
- [26] J. Walker, H. Ursic, A. Bencan, B. Malic, H. Simons, I. Reaney, G. Viola, V. Nagarajan, T. Rojac, Temperature dependent piezoelectric response and strain-electric-field hysteresis of rare-earth modified bismuth ferrite ceramics. *J Mater Chem C.* 18–26 (2016).
- 350 [27] T. Rojac, H. Ursic, A. Bencan, B. Malic, D. Damjanovic, Mobile domain walls as a bridge between nanoscale conductivity and macroscopic electromechanical response. *Adv Funct Mater.* **25**, 2099–2108 (2015).
- [28] A. A. Esin, D. O. Alikin, A. P. Turygin, A. S. Abramov, J. Hreščak, J. Walker, T. Rojac, A. Bencan, B. Malic, A. L. Kholkin, V. Y. Shur, Dielectric relaxation and charged domain walls in (K,Na) NbO<sub>3</sub>-based ferroelectric ceramics. *J Appl Phys.* **121**, 74101 (2017).
- 355



- [29] M. I. Morozov, D. Damjanovic, Charge migration in  $\text{Pb}(\text{Zr,Ti})\text{O}_3$  ceramics and its relation to ageing, hardening, and softening. *J Appl Phys.* **107**, 1–10 (2010).
- [30] S. V. Kalinin, B. J. Rodriguez, S. Jesse, J. Shin, A. P. Baddorf, P. Gupta, H. Jain, D. B. Williams, A. Gruverman, Vector piezoresponse force microscopy. *Microsc Microanal.* **12**, 206 (2006).
- 360 [31] N. Balke, S. Jesse, P. Yu, B. Carmichael, S. V. Kalinin, A. Tselev, Quantification of surface displacements and electromechanical phenomena via dynamic atomic force microscopy. *Nanotechnology.* **27**, 42 (2016).
- [32] U. Rabe, K. Janser, W. Arnold, Vibrations of free and surface-coupled atomic force microscope cantilevers: Theory and experiment. *Rev Sci Instrum.* **67**, 3281 (1996).
- 365 [33] S. Hong, J. Woo, H. Shin, J. U. Jeon, Y. E. Pak, E. L. Colla, N. Setter, E. Kim, K. No, Principle of ferroelectric domain imaging using atomic force microscope. *J Appl Phys.* **89**, 1377–1386 (2001).
- [34] T. Jungk, Á. Hoffmann, E. Soergel, Quantitative analysis of ferroelectric domain imaging with piezoresponse force microscopy. *Appl Phys Lett.* **89**, 1–4 (2006).
- [35] E. Soergel, Piezoresponse force microscopy (PFM). *J Phys D Appl Phys.* **44**, 464003 (2011).
- 370 [36] E. A. Eliseev, A. N. Morozovska, A. V. Ievlev, Balke N, Maksymovych P, Tselev A, Kalinin SV: Electrostrictive and electrostatic responses in contact mode voltage modulated scanning probe microscopies. *Appl Phys Lett.* **104**, 232901 (2014).
- [37] H. Lu, C.-W. Bark, D. Esque de los Ojos, J. Alcala, C. B. Eom, G. Catalan, A. Gruverman, Mechanical writing of ferroelectric polarization. *Science.* **336**, 59–61 (2012).
- 375 [38] S. Jesse, A. P. Baddorf, S. V. Kalinin, Switching spectroscopy piezoresponse force microscopy of ferroelectric materials. *Appl Phys Lett.* **88**, 21–24 (2006).
- [39] R. K. Vasudevan, S. Jesse, Y. Kim, A. Kumar, S. V. Kalinin, Spectroscopic imaging in piezoresponse force microscopy: New opportunities for studying polarization dynamics in ferroelectrics and multiferroics. *MRS Commun.* **2**, 61–73 (2012).
- 380 [40] N. Balke, P. Maksymovych, S. Jesse, I. I. Kravchenko, Q. Li, S. V. Kalinin, Exploring local electrostatic effects with scanning probe microscopy: implications for piezoresponse force microscopy and triboelectricity. *ACS Nano.* **8**, 10229–10236 (2014).
- [41] Y. Kim, C. Bae, K. Ryu, H. Ko, Y. K. Kim, S. Hong, H. Shin, Origin of surface potential change during ferroelectric switching in epitaxial  $\text{PbTiO}_3$  thin films studied by scanning force microscopy. *Appl Phys Lett.* **94**, 032907 (2009).
- 385